Supporting Information

Cao et al. 10.1073/pnas.0913000107

SI Text

The supporting material includes the following:

- A mathematic analysis of water vapor response to CO_2-physiological and CO_2-radiative forcing.
- A discussion comparing this study with our previous study on the effect of CO_2-physiological forcing.
- Table S1 lists the climatic effect of CO_2-radiative, physiological, and combined radiative and physiological forcing for the fields not included in Table 1.
- Fig. S1 shows the temporal evolution of surface air temperature over the last 70-yr simulations (of the total 100-yr simulations) for each model experiment.
- Fig. S2 shows changes in canopy transpiration, canopy evaporation, and soil evaporation in response to the effect of CO_2-radiative forcing, CO_2-physiological forcing, and the combined CO_2-radiative and physiological forcing.
- Fig. S3 shows changes in planetary albedo, surface albedo, and snow cover in response to the effect of CO_2-radiative forcing, CO_2-physiological forcing, and the combined CO_2-radiative and physiological forcing.
- Fig. S4 shows changes in precipitation, evapotranspiration, and the difference between precipitation and evapotranspiration in response to the effect of CO_2-radiative forcing, CO_2-physiological forcing, and the combined CO_2-radiative and physiological forcing.
- Fig. S5 shows the percentage change in precipitable water in response to the effect of CO_2-radiative forcing, CO_2-physiological forcing, and the combined CO_2-radiative and physiological forcing.
- Fig. S6 shows changes in surface air temperature and runoff in response to the combined effect of CO_2-radiative and physiological forcing, and the linear sum of the effect of CO_2-radiative forcing and physiological forcing.
- Fig. S7 shows zonally averaged change in temperature and specific humidity in response to the effect of CO_2-radiative and physiological forcing.

Analysis of Water Vapor Response to CO_2-Radiative and CO_2-Physiological Forcing. Changes in atmospheric water vapor content can be expressed by the sum of water vapor change due to climate feedbacks and its change due to external sources/sinks, as shown by the following equation:

$$\Delta Q = \Delta Q_s + \Delta Q_f = \Delta Q_s + f \times Q_0 \times \Delta T \qquad \textbf{[S1]}$$

In the above equation, ΔQ is total change in water vapor content. ΔQ_s is water vapor change from external sources/sinks. ΔQ_f is the change in water vapor as a result of temperature-induced feedbacks, which can be expressed by the product of the initial amount of water vapor Q_0, the amount of temperature change (ΔT), and the fractional change in water vapor per degree of temperature change (f).

According to the Clausius-Clapeyron equation, the change in saturation water vapor pressure per degree of temperature change is calculated as:

$$\frac{de_s}{dT} = \frac{L_v e_s}{R_v T^2}, \qquad \textbf{[S2]}$$

where e_s is saturation water vapor pressure, T is temperature, L_v is latent heat of evaporation, and R_v is water vapor gas constant. The model control simulation has a global-mean surface temperature of 287.41 K, which corresponds to a saturation water vapor pressure (e_s) of 16.24 millibar (mb). Taking L_v to be $2.5 \times 10^6\ \mathrm{J\,kg^{-1}}$ and R_v to be $461.5\ \mathrm{J\,kg^{-1}\,K^{-1}}$, the calculation from the right hand side of Eq. **2** yields $de_s/dT = 1.065\ \mathrm{mb\,K^{-1}}$. In terms of percentage change, this corresponds to $6.56\%\ \mathrm{K^{-1}}$ for the change in saturation water vapor per degree of temperature change. By assuming a constant relative humidity (1, 2) under climate change, this number also applies to the change in atmospheric water vapor content per degree of temperature change, giving a value of $6.56\%\ \mathrm{K^{-1}}$ for f.

In the case of CO_2-radiative forcing, changes in water vapor are driven by temperature-induced feedbacks alone. Taking global-mean values from Table 1 and the value of $25.24\ \mathrm{kg\,m^{-2}}$ for precipitable water in the control simulation, water vapor change from the feedback term $\Delta Q_f = f \times Q_0 \times \Delta T = 0.0656\ \mathrm{K^{-1}} \times 25.24\ \mathrm{kg\,m^{-2}} \times 2.50\ \mathrm{K} = 4.14\ \mathrm{kg\,m^{-2}}$, which is close to the modeled water vapor increase of $4.28\ \mathrm{kg\,m^{-2}}$ in response to CO_2-radiative forcing. The small difference between the modeled value and what is determined from the Clausius-Clapeyron equation is a result of the small change in modeled relative humidity (0.38% increase).

In the case of CO_2-physiological forcing, change in water vapor is caused by two processes: on one hand, reduced canopy transpiration induces warming, which leads to an increase in water vapor content through temperature-water vapor feedback. This is the feedback term ΔQ_f. On the other hand, reduced canopy transpiration diminishes the source or atmospheric water vapor, which tends to decrease water vapor content. This is the external source/sink term ΔQ_s. Using values given in Table 1, the feedback term $\Delta Q_f = f \times Q_0 \times \Delta T = 0.0656\ \mathrm{K^{-1}} \times 25.24\ \mathrm{kg\,m^{-2}} \times 0.22\ \mathrm{K} = 0.36\ \mathrm{kg\,m^{-2}}$. This value is much larger than model-predicted water vapor increase of $0.19\ \mathrm{kg\,m^{-2}}$ in response to CO_2-physiological forcing, indicating that in addition to temperature-water vapor feedback, a diminished source for water vapor is operating in response to CO_2-physiological forcing. This diminished source is the reduced plant transpiration as a result of CO_2-physiological forcing.

Comparison Between This Study and Our Previous Study on the Effect of CO_2-Physiological Forcing That Used CLM3. In our previous study (3) using CLM3/CAM3.1 model it was reported that in response to a doubling of atmospheric CO_2, the warming over land caused by CO_2-physiological effect is only 0.12 K, which is much smaller than the 0.42 K warming simulated here using CAM3.5/CLM3.5. The much smaller warming is a result of unrealistic simulation of the partitioning in evapotranspiration. In the control simulation of CLM3/CAM3.1 canopy transpiration only accounts for 7% of evapotranspiration, whereas canopy and soil evaporation accounts for 71% and 22%, respectively. As a result, in response to the physiological effect of CO_2 doubling, the decrease in canopy transpiration in the CLM3/CAM3.1 simulation was largely offset by the increase in soil evaporation, and evapotranspiration decreases by only 0.2%. The negligible change in evapotranspiration explains the weak climate response to CO_2-physiological forcing from the simulations using CLM3/CAM3.1 (3).

Compared to CLM3, dramatic improvement in the simulation of surface hydrology is achieved in CLM3.5 through the implementation of new datasets and improved parameterizations for canopy interception, soil evaporation, and soil water availability (4). In particular, compared to CLM3, CLM3.5 has a more realistic simulation in its partitioning of global evapotranspiration with a significantly increased fractional contribution from canopy transpiration. In the control simulation of CLM3.5/CAM3.5, canopy transpiration, canopy evaporation, and soil evaporation account for 41%, 16%, and 43% of evapotranspiration, respectively. This modeled partitioning of evapotranspiration is consistent with the ensemble results from a broad range of land surface models (5) in which global evapotranspiration is dominated by canopy transpiration (48%), with substantially smaller contributions from canopy evaporation (16%) and soil evaporation (36%). In contrast to the study using CLM3/CAM3.1, increased soil evaporation in response to CO_2-physiological forcing in the simulation here using CLM3.5 only partly offsets decreased canopy transpiration, with 4% decrease in total evapotranspiration (Table S1). The large differences in the evapotranspiration response to CO_2-physiological forcing between this study and the previous one (3) explain the differences in simulated climate response to CO_2-physiological forcing between these two studies.

1. Allen MR, Ingram WJI (2002) Constraints on future changes in climate and the hydrological cycle. *Nature* 19:224–232 doi: 10.1038/nature01092.
2. Held IM, Soden BJ (2006) Robust responses of the hydrological cycle to global warming. *J Clim* 19:5686–5699.
3. Cao L, et al. (2009) Climate response to physiological forcing of carbon dioxide simulated by the coupled Community Atmosphere Model (CAM3.1) and Community Land Model (CLM3.0) *Geophys Res Lett* 36:L10402 doi: 10.1029/2009GL037724.
4. Oleson KW, et al. (2008) Improvements to the Community Land Model and their impact on the hydrological cycle *Journal of Geophys Res* 113:G01021 doi: 10.1029/2007JG000563.
5. Dirmeyer PA, et al. (2006) GSWP2: multimodel analysis and implications for our perception of the land surface *Bull Am Meteorol Soc* 87:1381–1397.

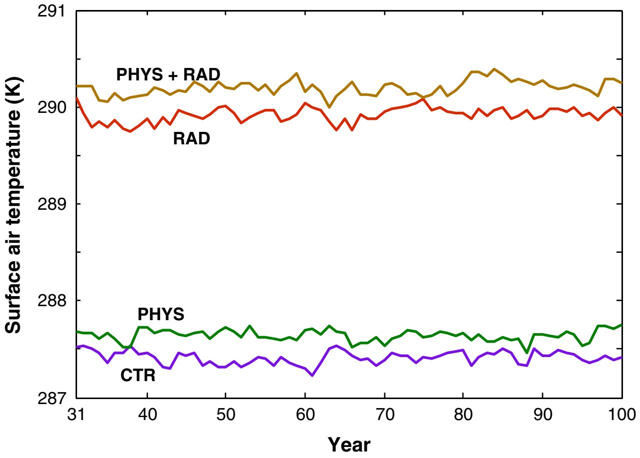

Fig. S1. Temporal evolution of surface air temperature over the last 70 yr of 100-yr model simulations (year 31 to year 100) for CTR (control), PHYS (CO_2-physiological forcing), RAD (CO_2-radiative forcing), and PHYS + RAD (combined radiative and physiological forcing) experiments. The trend in surface air temperature over the 70-yr period is 0.0, −0.0002, 0.0012, and 0.0014 K per year for CTR, PHYS, RAD, and PHYS + RAD simulations, respectively. The interannual variability during the 70-yr period as measured by standard deviation of the global-mean surface air temperature is 0.07 K for all of the four simulations.

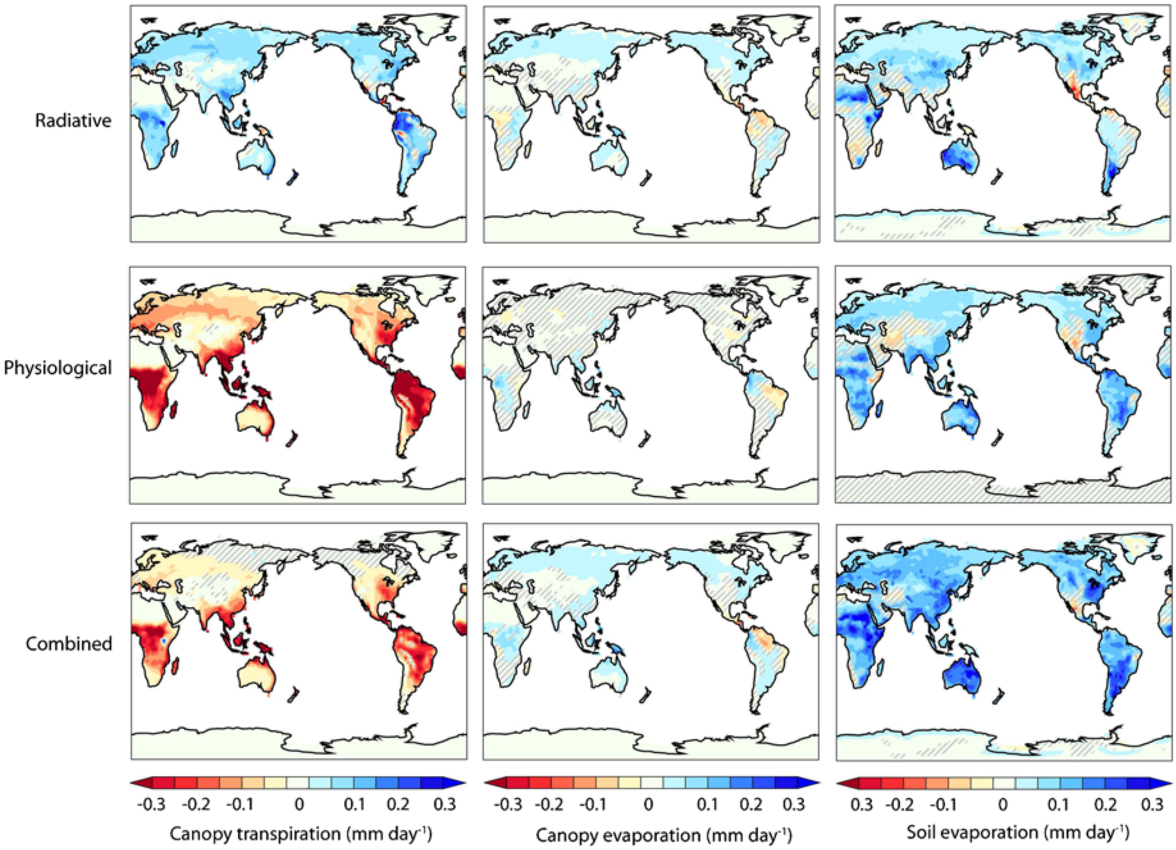

Fig. S2. Changes in canopy transpiration, canopy evaporation, and soil evaporation in response to the effect of CO_2-radiative forcing, CO_2-physiological forcing, and the combined CO_2-radiative and physiological forcing. All results shown here are annual mean changes in response to a doubling of atmospheric CO_2 calculated from the last 70-yr results of 100-yr simulations. Hatched areas are regions where changes are *not* statistically significant at the 5% level using the Student t-test.

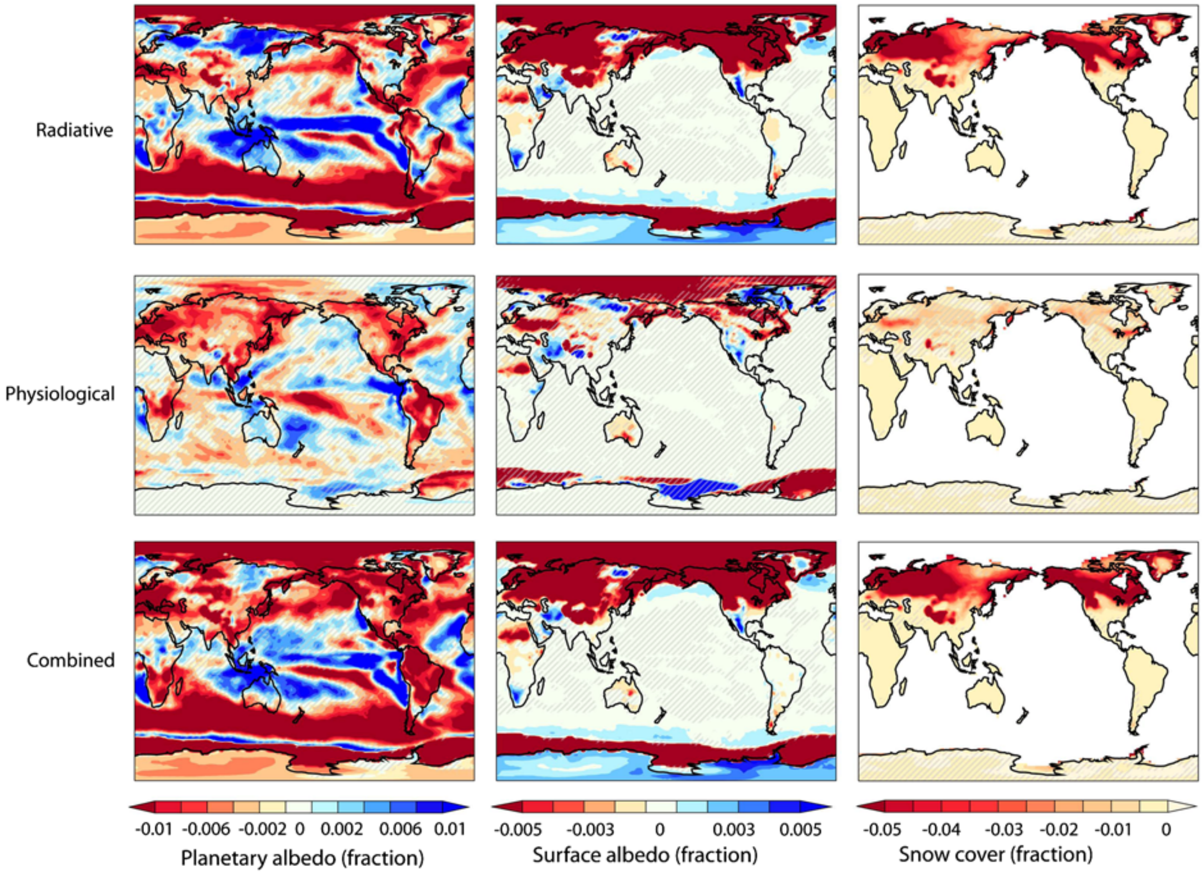

Fig. S3. Changes in planetary albedo, surface albedo, and snow cover in response to the effect of CO_2-radiative forcing, CO_2-physiological forcing, and the combined CO_2-radiative and physiological forcing. All results shown here are annual mean changes in response to a doubling of atmospheric CO_2 calculated from the last 70-yr results of 100-yr simulations. Hatched areas are regions where changes are *not* statistically significant at the 5% level using the Student t-test.

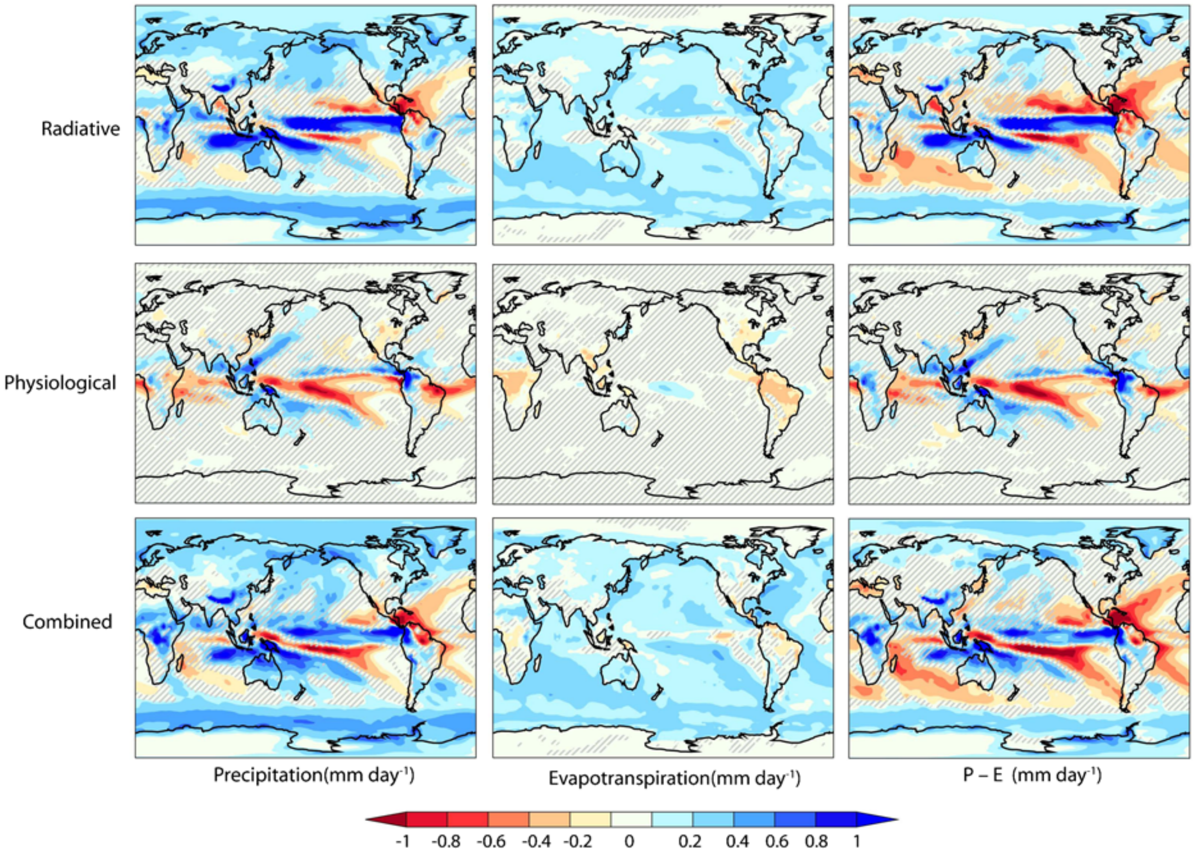

Fig. S4. Changes in precipitation, evapotranspiration, and the difference between precipitation and evapotranspiration (P–E) in response to the effect of CO_2-radiative forcing, CO_2-physiological forcing, and the combined CO_2-radiative and physiological forcing. All results shown here are annual mean changes in response to a doubling of atmospheric CO_2 calculated from the last 70-yr results of 100-yr simulations. Hatched areas are regions where changes are *not* statistically significant at the 5% level using the Student t-test.

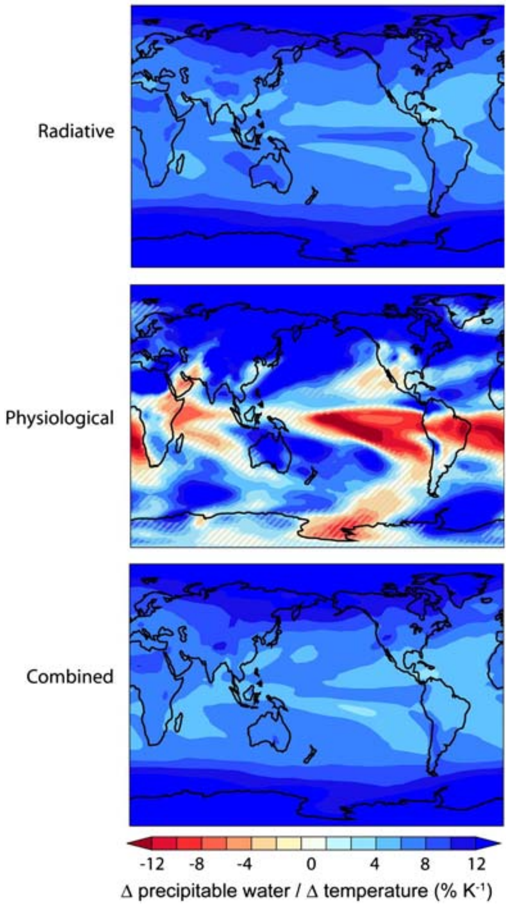

Fig. S5. Percentage change in precipitable water per degree of temperature change in response to the effect of CO_2-radiative forcing, CO_2-physiological forcing, and the combined CO_2-radiative and physiological forcing. All results shown here are annual mean changes in response to a doubling of atmospheric CO_2 calculated from the last 70-yr results of 100-yr simulations. Hatched areas are regions where changes are *not* statistically significant at the 5% level using the Student t-test. It is shown that in response to CO_2-radiative forcing, the change in precipitable water per degree of temperature change is rather uniform with a global-mean value of 6.7% per degree of warming, suggesting that water vapor change follows the Clausius-Clapeyron formula that governs the relationship between temperature and water vapor. However, in response to CO_2-physiological forcing, the change in precipitable water is more heterogeneous. Some regions, such as the Amazon, experience a reduction in precipitable water in spite of increase in surface air temperature. This reduction in precipitable water suggests that in addition to temperature-induced feedbacks, water vapor change in association with CO_2-physiological forcing is strongly controlled by its diminished source from reduced canopy transpiration.

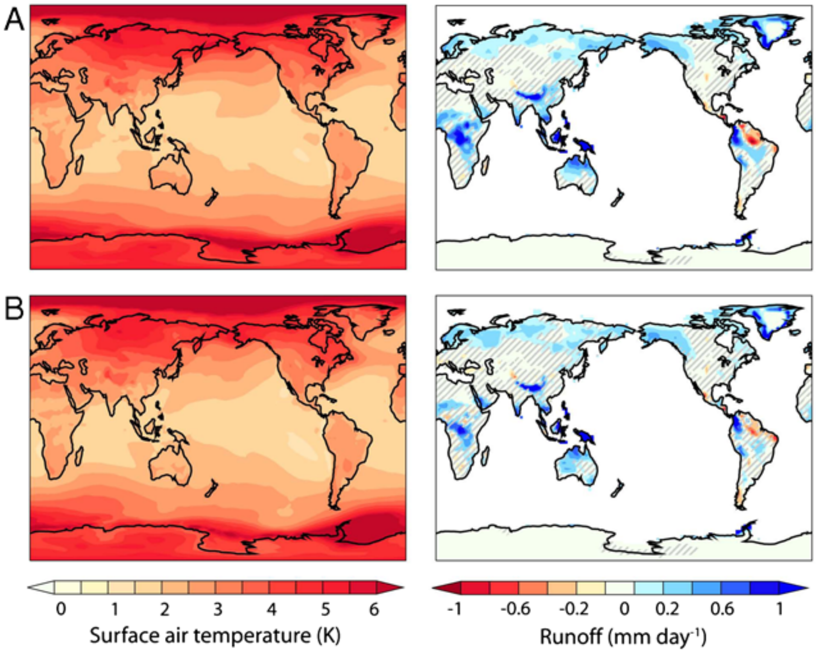

Fig. S6. Changes in surface air temperature and runoff in response to the combined effect of CO_2-radiative and physiological forcing (*A*), and the linear sum of the effect of CO_2-radiative and physiological forcing (*B*). All results shown here are annual mean changes in response to a doubling of atmospheric CO_2 calculated from the last 70-yr results of 100-yr simulations. It is shown that the combined effect of CO_2-radiative and physiological forcing can be well represented by the linear sum of these two effects.

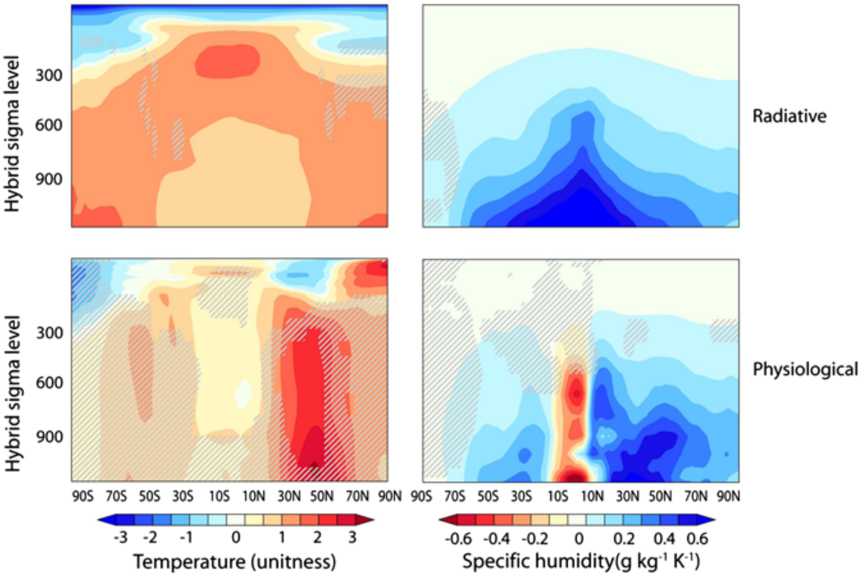

Fig. S7. Zonally averaged change in temperature and specific humidity in response to the effect of CO_2-radiative forcing and physiological forcing. All values are normalized by changes in global-mean surface air temperature for CO_2-radiative forcing (2.50 K) or CO_2-physiological forcing (0.22 K). All results shown here are annual mean changes in response to a doubling of atmospheric CO_2 calculated from the last 70-yr results of 100-yr simulations. To avoid errors due to interpolation, we did not perform any vertical interpolation in the vertical and hence the vertical axis is the model's hybrid-sigma coordinate (increase in height upward). Hatched areas are regions where changes are *not* statistically significant at the 5% level using the Student t-test.

Table S1. Climate responses to CO_2-radiative forcing, CO_2-physiological forcing, and combined CO_2-radiative and physiological forcing for fields not listed in Table 1.

	RAD − CTR	PHYS − CTR	RAD + PHYS − CTR
Photosynthesis (%)	−1.02 ± 0.10	31.22 ± 0.14	30.6 ± 0.15
Sunlit stomatal resistance (%)	0.58 ± 0.06	2.32 ± 0.07	2.80 ± 0.08
Shaded stomatal resistance (%)	0.65 ± 0.07	3.89 ± 0.07	4.49 ± 0.08
Canopy evaporation (%)	4.17 ± 0.23	0.91 ± 0.23	4.17 ± 0.23
Canopy transpiration (%)	6.85 ± 0.14	−18.83 ± 0.13	−12.31 ± 0.13
Soil evaporation (%)	5.56 ± 0.38	8.94 ± 0.36	15.24 ± 0.37
Total evapotranspiration (%)	5.64 ± 0.20	−3.80 ± 0.17	2.25 ± 0.20
Total cloudiness (fraction)	0.0057 ± 0.0003	−0.0009 ± 0.0003	0.0048 ± 0.0003
Total cloudiness over land (fraction)	0.0055 ± 0.0007	−0.0043 ± 0.0006	0.0012 ± 0.0007
Shortwave cloud forcing (Wm^{-2})	−0.62 ± 0.04	0.42 ± 0.04	−0.15 ± 0.04
Shortwave cloud forcing over land (Wm^{-2})	−0.50 ± 0.07	1.30 ± 0.07	0.85 ± 0.07
Longwave cloud forcing (Wm^{-2})	−0.32 ± 0.01	−0.03 ± 0.01	−0.34 ± 0.01
Longwave cloud forcing over land (Wm^{-2})	−0.20 ± 0.06	0.23 ± 0.05	0.09 ± 0.06

RAD − CTR represents the effect of CO_2-radiative forcing; PHYS − CTR represents the effect of physiologcial forcing; RAD + PHYS − CTR represents the combined effect of CO_2-radiative and physiological forcing. All results are annual mean values averaged from the last 70-yr results of 100-yr simulations. Uncertainties are represented by ±1 standard error calculated from the last 70-yr results of 100-yr simulations.